Math and Computer Science Faculty Publications   Math and Computer Science

2009

Complementary responses to mean and variance modulations in the perfect integrate-and-fire model

Joanna R. Wares
University of Richmond, jwares@richmond.edu

Todd W. Troyer

Follow this and additional works at: http://scholarship.richmond.edu/mathcs-faculty-publications

Part of the Mathematics Commons, and the Neurosciences Commons

This is a pre-publication author manuscript of the final, published article.

Joanna Pressley · Todd W. Troyer

Complementary responses to mean and variance modulations in the perfect integrate-and-fire model.

Abstract In the perfect integrate-and-fire model (PIF), the membrane voltage is proportional to the integral of the input current since the time of the previous spike. It has been shown that the firing rate within a noise free ensemble of PIF neurons responds instantaneously to dynamic changes in the input current, whereas in the presence of white noise, model neurons preferentially pass low frequency modulations of the mean current. Here, we prove that when the input variance is perturbed while holding the mean current constant, the PIF responds preferentially to high frequency modulations. Moreover, the linear filters for mean and variance modulations are complementary, adding exactly to one. Since changes in the rate of Poisson distributed inputs lead to proportional changes in the mean and variance, these results imply that an ensemble of PIF neurons transmits a perfect replica of the time-varying input rate for Poisson distributed input. A more general argument shows that this property holds for any signal leading to proportional changes in the mean and variance of the input current.

1 Introduction

In the simplest of the integrate-and-fire models, the perfect integrate-and-fire (PIF) model, the membrane voltage is driven exclusively by external currents. With leak channels omitted, capacitive integration causes the membrane voltage to be perfectly proportional to the integral of the input current since the last spike. The simplicity of the model allows the derivation of closed form solutions in many instances (Knight 1972; Stein et al 72; Abbott and van Vreeswijk 1993; Salinas and Sejnowski 2002; Lindner 2004).

Joanna Pressley
Vanderbilt University
E-mail: j.pressley@vanderbilt.edu

Todd W. Troyer
University of Texas, San Antonio

In his seminal work, Knight (1972) determined the firing rate response of the PIF to deterministic input. Knight first defined the firing rate as the inverse of the interval between two spikes in a single neuron. Under this definition, the firing rate response to small perturbations of the input current is proportional to the input perturbation averaged over the baseline inter-spike interval, T_0. This averaging causes the PIF to act as a low-pass filter and for the gain to go to zero when the period of the input is a multiple of T_0. Knight then analyzed the response dynamics of a large ensemble of PIF neurons, defining firing rate as the spike probability per unit time across the ensemble. In contrast to the inter-spike interval definition, the ensemble firing rate was an exact scaled replica of the input signal.

More recently, Fourcaud and Brunel (2002) analyzed ensembles of PIF neurons in the presence of white noise inputs, using methods introduced by Gerstein and Mandelbrot (1964). They showed that the linear response to small perturbations in the mean current was low-pass, dropping to zero for input modulations significantly faster than $\sigma^2/2\mu^2$, where σ^2 is the variance and μ is the mean of the input current at baseline.

But under the rate coding hypothesis, the ultimate goal is to understand how neural populations transform input rates to output rates; parameters describing the input current are just intermediate variables. Under the assumption that the dominant origin of neuronal noise is synaptic (Calvin and Stevens 1967; Dodge et al 1968), we expect both the mean *and* the variance to be strongly dependent on pre-synaptic firing rate. For example, for Poisson-distributed pre-synaptic spike trains, changes in the variance of the current are proportional to changes in the mean. If we separate the input into excitatory and inhibitory components, balanced changes will modulate the variance of the synaptic current while causing relatively minor changes in the mean, whereas a push-pull interaction of excitation and inhibition will cause large changes in the mean current but relatively minor changes in the variance (Abbott and Chance 2005). Thus, it is possible to transmit signals using modulations in input

variance as well as modulations in the mean (Lindner and Schimansky-Geier 2001; Silberberg et al 2004; Fourcaud-Trocmé and Brunel 2005). In this work, we derive the linear response of the PIF for modulations of the input variance, and show that this is exactly complementary to the linear response to modulations in the mean. We also show that proportional changes in the mean and variance lead to output firing rates that perfectly replicate modulations in the input.

2 Model

The starting point for the model is a pattern of synaptic input consisting of a series of instantaneous current pulses:

$$I_s(t) = \sum_k \overline{Q}\delta(t - t^k). \tag{1}$$

$\overline{Q}$ is the total charge carried by one input and δ is the Dirac delta function. The arrival times of pre-synaptic spikes, t^k, are assumed to be generated by a Poisson process with average rate $\lambda(t)$. The current is then a stochastic process whose time varying mean is given by $\mu(t) = \overline{Q}\lambda(t)$ and whose variance $\sigma^2(t) = \overline{Q}^2\lambda(t)$. This variance, which has units of charge^2/time can be thought of as the rate of the accumulation in charge variance.

If synaptic inputs are instantaneous, weak, and uncorrelated in time, we can adopt a diffusion approximation, and consider the stochastic PIF:

$$C\frac{dV}{dt} = \mu(t) + \sigma(t)\eta(t), \tag{2}$$

where C is the membrane capacitance, V is the membrane potential, and $\eta(t)$ is Gaussian white noise process ($\langle\eta(t)\rangle = 0$ and $\langle\eta(t)\eta(t')\rangle = \delta(t - t')$) (Ricciardi 1977). A spike is generated when the voltage reaches a threshold value V_θ, after which the voltage is reset to V_r. To facilitate the analysis, we assume that the spike and reset process is instantaneous.

Instead of directly tracking individual trajectories, we adopt the Fokker-Planck (forward Kolmogorov) formalism and study the dynamics of the density $\rho(V, t)$ that describes the probability that a given trajectory is near the voltage V at time t (Gerstein and Mandelbrot 1964; Ricciardi 1977; Tuckwell 1988; Nykamp and Tranchina 2000; Fourcaud and Brunel 2002). For any given voltage the net flux or "rate of flow" $J_V(V, t)$ across that voltage can be calculated as

$$J_V(V, t) = -\frac{\sigma^2(t)}{2C^2}\frac{\partial\rho(V, t)}{\partial V} + \frac{\mu(t)}{C}\rho(V, t). \tag{3}$$

The probability density function (PDF) obeys the following dynamics:

$$\frac{\partial\rho(V, t)}{\partial t} = \frac{-\partial J_V(V, t)}{\partial V} \tag{4}$$

$$\frac{\partial\rho}{\partial t} = \frac{\sigma^2}{2C^2}\frac{\partial\rho^2}{\partial^2 V} - \frac{\mu}{C}\frac{\partial\rho}{\partial V}. \tag{5}$$

The first term on the right-hand side is the diffusion term, which describes how the ensemble's voltage distribution spreads due to noise. The second term describes how the mean level of input forces the distribution left or right and is often called the drift or driving force. In this framework, the ensemble firing rate is equal to the flux crossing threshold:

$$r(t) = J_V(V_\theta, t). \tag{6}$$

To model the spike and reset mechanism, the flux crossing threshold is re-injected at the reset voltage V_r.

3 Perturbations of the Variance

Previous work has produced solutions for the probability density function when μ and σ are held constant (Abbott and van Vreeswijk 1993), as well as time-dependent solutions for sinusoidal perturbations in μ (Fourcaud and Brunel 2002). Here we extend the latter derivation to examine the response dynamics of the PIF when the input variance is perturbed by sinusoids of frequency ω and amplitude $\epsilon\sigma_0^2$ (complex notation is used to simplify calculations):

$$\sigma^2(t) = \sigma_0^2(1 + \epsilon\exp(i\omega t)). \tag{7}$$

To simplify notation, we change variables to a normalized (unit-less) membrane voltage u:

$$u = \frac{2\mu_0 VC}{\sigma_0^2}. \tag{8}$$

The Fokker-Planck equation becomes

$$\tau_e\frac{\partial\rho(u, \omega)}{\partial t} = (1 + \epsilon\exp(i\omega t))\frac{\partial\rho^2}{\partial^2 u} - \frac{\partial\rho}{\partial u}, \tag{9}$$

where $\tau_e = \sigma_0^2/(2\mu_0^2)$. Since σ_0^2 has units of charge^2 per time and μ has units of charge per time, τ_e has units of time and hence sets a characteristic timescale for the PIF.

The boundary conditions in the new variables are as follows:

To prevent an infinite value of the flux, the density must be continuous both at threshold and spike reset,

$$\rho(u_\theta, t) = 0 \tag{10}$$

$$\rho(u_{r_-}, t) = \rho(u_{r_+}, t). \tag{11}$$

The firing rate is given as the flux across threshold, and this flux is injected back at the reset voltage u_r,

$$\frac{d\rho}{du}(u_\theta, t) = -r(t)\tau_e \tag{12}$$

$$\frac{d\rho}{du}(u_{r_+}, t) - \frac{d\rho}{du}(u_{r_-}, t) = -r(t)\tau_e. \tag{13}$$

Finally, the integrated probability must be equal to one,

$$\int_{-\infty}^{u_\theta} \rho(u, t)du = 1. \tag{14}$$

To characterize the first order response, $\rho(u, \omega, t)$ and $r(t)$ are expanded in orders of ϵ (assumed to be small):

$$\rho(u, \omega, t) = \rho_0(u) + \epsilon \exp(i\omega t)\widehat{\rho}(u, \omega) + O(\epsilon^2) \tag{15}$$

$$r(t) = r_0(1 + \epsilon \exp(i\omega t)\widehat{r}_{\sigma^2}(\omega)) + O(\epsilon^2) \tag{16}$$

where the complex quantities $\widehat{\rho}(u, \omega)$ and $\widehat{r}_{\sigma^2}$ determine the amplitude and phase of the first order response relative to input. We then plug the approximation (15) into the Fokker-Planck equation (9) and the boundary conditions (10-14), and separate the terms into two sets of equations. The solution to the first set of equations describes the steady-state PDF and response (ρ_0 and r_0). The solution to the second set of equations describes the dynamics of the PIF's response to the sinusoidal component of variance that is first order in ϵ ($\widehat{\rho}$ and $\widehat{r}_{\sigma^2}$).

The steady state solution is given by (Abbott and van Vreeswijk 1993)

$$\rho_0 = r_0\tau_e[1 - \exp(u - u_\theta - \Theta(u_r - u)(1 - \exp(u - u_r)))], \tag{17}$$

where $\Theta(x)$ is the Heaviside function that steps from a value of 0 to 1 at $x = 0$. The first order equation for $\widehat{\rho}$ is a nonhomogeneous ordinary differential equation:

$$\frac{d^2\widehat{\rho}}{du^2} - \frac{d\widehat{\rho}}{du} - i\tau_e\omega\widehat{\rho} = -\frac{d^2\rho_0}{du^2}. \tag{18}$$

To determine the first order modulations in firing rate, we find a particular solution to (18), and add to this the class of general solutions to the corresponding homogeneous equation

$$\frac{d^2\widehat{\rho}}{du^2} - \frac{d\widehat{\rho}}{du} - i\tau_e\omega\widehat{\rho} = 0. \tag{19}$$

The final solution is determined by satisfying the first order boundary conditions derived from (10)-(14):

$$\widehat{\rho}(u_\theta) = 0 \tag{20}$$

$$\widehat{\rho}(u_{r_+}) = \widehat{\rho}(u_{r_-}) \tag{21}$$

$$\frac{\partial\rho_0}{\partial u}(u_\theta) + \frac{\partial\widehat{\rho}}{\partial u}(u_\theta, \omega) = -r_0\widehat{r}_{\sigma^2}(\omega)\tau_e \tag{22}$$

$$\frac{\partial\rho_0}{\partial u}(u_{r_+}) - \frac{\partial\rho_0}{\partial u}(u_{r_-}) + \frac{\partial\widehat{\rho}}{\partial u}(u_{r_+}, \omega) - \frac{\partial\widehat{\rho}}{\partial u}(u_{r_-}, \omega) \tag{23}$$
$$= -r_0\widehat{r}_{\sigma^2}(\omega)\tau_e$$

$$\int_{-\infty}^{u_\theta} \widehat{\rho}(u, \omega)du = 0. \tag{24}$$

Following (Fourcaud and Brunel 2002), we guess that the particular solution has the form $\widehat{\rho}_p = K\frac{\partial\rho_0}{\partial u}$. Plugging this into (18) and using the fact that $\frac{\partial^n\rho_0}{\partial u^n} = \frac{\partial\rho_0}{\partial u}$ for $n > 1$, we find

$$i\tau_e\omega K\frac{\partial\rho_0}{\partial u} = \frac{\partial\rho_0}{\partial u} + K\frac{\partial\rho_0}{\partial u} - K\frac{\partial\rho_0}{\partial u}. \tag{25}$$

So $K = \frac{1}{i\omega\tau_e}$ and the particular solution is given by

$$\widehat{\rho}_p = \frac{1}{i\omega\tau_e}\frac{\partial\rho_0}{\partial u}. \tag{26}$$

To find the general solution of the homogenous equation (19), we assume that the solution is of the form $\exp(z(\omega)u)$, and find:

$$z^2 - z - i\omega\tau_e = 0 \tag{27}$$

$$z_\pm(\omega) = \frac{1 \pm \sqrt{1 + 4i\omega\tau_e}}{2}. \tag{28}$$

The general solutions to the homogeneous equation are given by

$$c_1\exp(z_+(\omega)u) + c_2\exp(z_-(\omega)u). \tag{29}$$

To satisfy the boundary conditions, some algebra (see the appendix) reveals that the solution for $\widehat{\rho}$ is

$$\widehat{\rho} = \frac{r_0}{i\omega}[-\exp(u - u_\theta) + \Theta(u_r - u)\exp(u - u_r) + \exp(z_+(\omega)(u - u_\theta)) - \Theta(u_r - u)\exp(z_+(\omega)(u - u_r))]. \tag{30}$$

Additionally, the boundary conditions allow us to find the solution for the first order firing rate modulation $\widehat{r}_{\sigma^2}(\omega)$, which is given by

$$\widehat{r}_{\sigma^2}(\omega) = 1 - \frac{\sqrt{1 + 4i\omega\tau_e} - 1}{2i\omega\tau_e}. \tag{31}$$

3.1 Gain and Phase of the Response

The complex valued response function $\widehat{r}_{\sigma^2}(\omega)$ describes the filter that transforms an input modulation $\epsilon\exp(\omega t)$ into the first order output response $r_0\epsilon\exp(i\omega t)\widehat{r}_{\sigma^2}$. The magnitude of $\widehat{r}_{\sigma^2}(\omega)$ is the gain of the filter, and the angle of $\widehat{r}_{\sigma^2}(\omega)$ is the phase shift. A plot of gain as a function of frequency shows that the PIF has low gain, and hence weak responses to low frequency modulations in the input variance and strong responses to high frequency modulations, i.e. the PIF acts like a high-pass filter (figure 1). The phase shift approaches zero at high frequencies. However, for low frequency modulations, the phase lead approaches 90°. The phase lead suggests that the PIF is responding to increases in the input variance.

The cutoff frequency is commonly defined as the frequency where the power of the response is $\frac{1}{2}$ of its maximum value. Since power is proportional to the square of

a voltage signal, the cutoff frequency is determined by finding the frequency that results in a gain equal to $\frac{1}{\sqrt{2}}$ (the maximum gain is 1). Since the frequency ω always enters the expression for the filter in terms of $\omega\tau_e$, the gain will be constant for $\omega = c/\tau_e$ for any constant c. For variance modulations, the gain is equal to $\frac{1}{\sqrt{2}}$ for $c = 4.24$. At this frequency, the phase shift is $19.5°$.
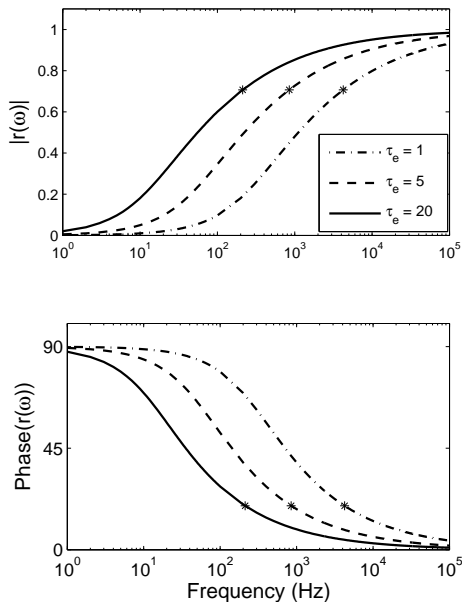
Fig. 1 Gain and phase curves for the PIF model due to perturbations in the variance. Asterisks mark the natural cutoff of the filter $\omega = \frac{4.24}{\tau_e}$.

4 Complementarity Between Mean and Variance Filtering

Fourcaud and Brunel (2002) previously used a similar derivation (see appendix) to show that perturbations in the mean current with variance held constant lead to firing rate modulations with the gain and phase given by the function

$$\widehat{r}_\mu(\omega) = \frac{\sqrt{1 + 4i\omega\tau_e} - 1}{2i\omega\tau_e}. \tag{32}$$

A comparison of equation (59) with equation (31) reveals that

$$\widehat{r}_\mu(\omega) + \widehat{r}_{\sigma^2}(\omega) = 1. \tag{33}$$

Thus, the filters for modulations in the mean and variance of the input are exactly complementary in that the sum of the two filters equals one (figure 2).

Note that the complementarity of the filters exists in the complex plane. While this implies that the gain of two filters need not add exactly to one, it is true that the filtering of modulations in the mean and variance are low and high-pass respectively. The single parameter τ_e determines the cutoff frequency marking the transition between the two filters. The gain curves intersect where the gain equals 0.58 and at a frequency given by $\omega = c/\tau_e$ with $c = 1.73$. Complementarity in the complex plane also means that the phases of the two filters only sum exactly to zero when the gain curves intersect. At this point the phase lag/lead is $30°$. However, complementarity does imply that the phases must have opposite sign, i.e. if responses to the mean show a lag at a given frequency, then the response to changes in the variance must show a phase lead.
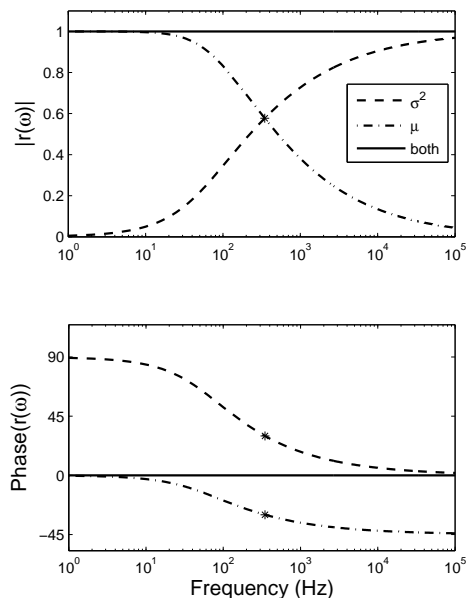
Fig. 2 Gain and phase curves for the PIF model due to perturbations in the mean and variance. The PIF model acts like a low-pass filter for mean changes and a high-pass filter for variance changes. The two filters are exactly complementary, summing to 1 at all frequencies.

The general shape of the each filter stems from the multiplicative nature of the firing rate equation (the flux over threshold). At threshold, the flux, J_V, is given by

$$J_V(\theta, t) = \frac{\sigma^2(t)}{2C^2}\left(-\frac{\partial\rho}{\partial V}(\theta, t)\right), \tag{34}$$

since $\rho(\theta) = 0$. Because the boundary conditions constrain the density ρ to equal zero at threshold, the steepness of the decline toward zero determines the total probability that the voltage falls in a boundary layer near

threshold. Therefore, equation (34) implies that the firing rate is proportional to the instantaneous value of the input variance multiplied by the accumulated probability that the membrane voltage lies near threshold. For fixed variance, the first term is fixed and an increase in the mean current increases the firing rate by pushing more trajectories toward threshold. Since this buildup will take time to accumulate, the response to changes in the mean are low pass. Conversely, a step increase in the input variance will immediately increase the firing rate. However, this increase in firing rate will cause a depletion in the density of trajectories near threshold. This depletion in turn will lead to a decay of firing rate until it matches the flux of probability flowing in to the boundary layer near threshold. Thus, the response to the change in variance is high pass. In the PIF model, both the mean and the variance of the input current are voltage independent and these near-threshold dynamics determine the firing rate response.

5 Response to a Proportional Change in Mean and Variance

Thus far, we have analyzed the filter that transforms modulations in the mean and variance of the input current to modulations in the ensemble firing rate. But if we assume that neural information is carried by firing rate, then the key transformation is from the rate of synaptic input, to the rate of spike output. The statistics of the input current simply characterize one step along this more fundamental transformation.

If we assume that the PIF model receives input from a single train of input spikes that are Poisson distributed, then the mean and variance of the current arising from these inputs are proportional: $\mu(t) = \overline{Q}\lambda(t)$ and $\sigma^2(t) = \overline{Q}^2\lambda(t)$.

Following the approach of the previous sections, consider sinusoidal modulations in Poisson input rate that lead to proportional modulations in the mean and variance of the input current.

$$\lambda(t) = \lambda_0^2(1 + \epsilon \exp(i\omega t)). \tag{35}$$

For small modulations, the perturbations of the output rate caused by the mean and variance modulations add linearly, and the firing rate filtering is just the sum of the mean and variance filters:

$$\widehat{r}(\omega) = \widehat{r}_\mu(\omega) + \widehat{r}_{\sigma^2}(\omega) = 1. \tag{36}$$

This argument demonstrates that the PIF model proportionally transmits small modulations in input rate for a single train of Poisson inputs.

This is a special case of a much more general result. For *any* proportional modulation of the mean and variance, we can write $\sigma^2(t) = as(t)$ and $\mu(t) = bs(t)$ where $s(t)$ is a positive signal and a and b are constants. The

argument does not take a perturbation approach, and changes in $s(t)$ need not be small.

The Fokker-Planck equation that describes the change in the p.d.f due to the signal $s(t)$ is then

$$s(t)^{-1}\frac{\partial\rho}{\partial t} = \frac{a}{2C^2}\frac{\partial^2\rho}{\partial V^2} - \frac{b}{C}\frac{\partial\rho}{\partial V}. \tag{37}$$

We define $T = \int_0^t s(t')dt'$. Because $s(t)$ is positive, the relationship between T and t is invertible, and we can view this transformation as a rescaling of time. Under this re-scaling,

$$s(t)^{-1}\frac{\partial}{\partial t} = \frac{\partial}{\partial T}, \tag{38}$$

and the Fokker-Planck equation is now

$$\frac{\partial\rho}{\partial T} = \frac{a}{2C^2}\frac{\partial^2\rho}{\partial V^2} - \frac{b}{C}\frac{\partial\rho}{\partial V}. \tag{39}$$

But this is just the equation for the PIF with a constant mean and variance. The equilibrium distribution ρ_0 is given by equation (17) and is determined by the ratio of the variance and the mean current $\tau_e = \sigma^2/2\mu = a/2b$ Abbott and van Vreeswijk (1993). This implies that proportional changes in the mean and variance do not alter the shape of the underlying p.d.f. of the voltage.

To determine the firing rate, we examine the flux at threshold

$$J_V(\theta) = \frac{\sigma^2}{2C^2}\left(-\frac{\partial\rho_0}{\partial V}(\theta)\right). \tag{40}$$

Since the voltage distribution does not change and the signal is proportional to the variance, it follows that the output firing rate is a proportional replica of the input signal $s(t)$.

6 Discussion

Knight (1972) previously demonstrated that the ensemble response of the PIF model perfectly replicates deterministic modulations in the input current. Subsequent research has shown that the addition of constant amplitude diffusive noise causes the PIF model to act like a low-pass filter (Fourcaud and Brunel 2002). Here, we have shown that in response to perturbations of the variance for constant mean input, the PIF acts like a high-pass filter. Moreover, the response to mean modulations and variance modulations are exactly complementary, with the two filter functions summing to one.

A primary motivation for studying simple models is that the clarity of the analytic results provides insight into the biophysical mechanisms that govern the properties of real neurons. High-pass filtering of modulations in the input variance has been shown for several integrate-and-fire type models (Fourcaud-Trocmé and Brunel 2005; Naundorf et al 2005), and has also been demonstrated

in real neurons using somatic current injection in vitro (Silberberg et al 2004). In the PIF model, we have shown that filtering of modulations in the mean and variance of input currents are complementary, and this complementarity is unaltered by cutoff frequencies changing in response to alterations in the relative magnitude of the noise.

The degree to which this complementarity generalizes to more realistic models and to real neurons is an open question. With the addition of a leak current, response resonances exist at integer multiples of the baseline firing rate (Knight 1972; Plesser and Geisel 1999; Brunel et al 2001; Fourcaud and Brunel 2002; Troyer 06), and these resonances will disrupt response complementarity. Furthermore, the leaky integrate-and-fire model (LIF) model can operate in a regime in which the mean input current is subthreshold and spikes result from occasional noise-driven fluctuations in the membrane voltage (Abeles 1991; Troyer and Miller 1997). Firing rates then depend on both the mean and the variance in the steady state, and can display complex resonances to modulations in input variance (Lindner and Schimansky-Geier 2001). Depending on LIF parameters, these factors complicate the relationship between the filtering of mean and variance modulations in ways that violate the exact complementarity seen in the PIF model. A full exploration of these effects is beyond the scope of this paper.

Within the framework of the rate encoding hypothesis, modulations in the statistics of the synaptic current are simply intermediate stages in the more fundamental transformation from input rates to output rates. However, we know of no studies directly characterizing transformations from time-varying rates to spike probability in real neurons. In the PIF model, a single train of rate-modulated Poisson inputs will induce proportional changes in the mean and variance of the input current. For small modulations, complementarity of the filters for mean and variance modulations can be used to show that the PIF model produces rate responses that are a scaled replica of the Poisson input rate. This argument is actually a special case of a much more general argument demonstrating that, as long as the diffusion approximation is valid, firing rates in the stochastic PIF model replicate *any* input signal in which the mean and variance of the input current change proportionally.

Although a single Poisson source leads to proportional scaling of the mean and variance, the two input variables become decoupled when considering both excitatory and inhibitory inputs (Miller and Troyer 2002; Abbott and Chance 2005). In the simplest case, adding an exact balance of excitation and inhibition to a baseline pattern of input will increase input variance while leaving the mean unchanged. Alternatively, changing the ratio of excitatory to inhibitory inputs while fixing the total rate of synaptic inputs will change the mean but not the variance of the input current. Complementary filters for the mean and variance suggest that neural signals carried by balanced inputs will be subject to high-pass filtering whereas inputs that result in a 'push-pull' trade-off between excitation and inhibition will be subject to low-pass filtering.

Traditionally, it has been assumed that firing rate is a function of an underlying 'generator potential' (Granit 1947; Katz 1950; Fuortes 1959), and hence response dynamics are low-pass due to capacitive filtering of membrane currents (Knight et al 70; Wilson and Cowan 1973; Carandini et al 1996). Others have shown that responses can be much faster than the membrane time constant, and have argued that synaptic filtering is the rate-limiting step for neural responses (Frolov and Medvedev 1986; Brunel and Hakim 1999; Koch 1999; Brunel et al 2001). Yet others have focused on the refractory period as the key timing parameter (Wilson and Cowan 1973; Abeles 1991). Our analysis of the PIF model suggests that the response time of neurons is also affected by relative magnitude of the mean and variance of synaptic input, a quantity that is not directly tied to a specific underlying biophysical timescale. Future research will be required to understand how timescales emerging from stochastic integration interact with the rich array of synaptic and membrane dynamics encountered in more realistic models of neural spiking.

7 Appendix

7.1 Perturbations of the Variance

The full solution for the nonhomogeneous equation (equation 18) is determined by choosing the correct constants for solutions to the homogeneous equation (19) which, when added to the particular solution (26), satisfy the boundary conditions (equations 20-24). Since the derivative of the solution is discontinuous at reset, the solution is determined on two intervals separately: the interval from u_r to u_θ and the interval from $-\infty$ to u_r. Letting $d_1 \exp(z_+ u) + d_3 \exp(z_-(\omega)u)$ and $d_2 \exp(z_+ u) + d_4 \exp(z_-(\omega)u)$ be the solutions to the homogeneous solution on these two intervals, the general solution to equation 18 has the form,

$$\widehat{\rho} = \frac{r_0}{i\omega}[-\exp(u-u_\theta)] + d_1 \exp(z_+(\omega)u) + d_3 exp(z_-(\omega)u),$$
$$u_r \leq u \leq u_\theta$$
$$\widehat{\rho} = \frac{r_0}{i\omega}[-\exp(u-u_\theta) + \exp(u-u_r)] +$$
$$d_2 \exp(z_+(\omega)u) + d_4 \exp(z_-(\omega)u), \quad u \leq u_r \quad (41)$$

Since the real part of $z_-(\omega)$ is negative, $d_4 = 0$ to ensure the integrability of ρ on the interval $u \leq u_r$. To simplify the remaining calculations, we let $k = r_0/i\omega$ and

make the following reassignments:

$$d_1 = k \ c_1 \exp(-z_+(\omega)u_\theta) \qquad (42)$$

$$d_2 = k \ c_1 \exp(-z_+(\omega)u_\theta) + kc_2 \exp(-z_+(\omega)u_r) \qquad (43)$$

$$d_3 = k \ c_3 \exp(-z_-(\omega)u_\theta). \qquad (44)$$

The general solution is then given by

$$\widehat{\rho} = k[-\exp(u - u_\theta) + c_1 \exp(z_+(\omega)(u - u_\theta)) \\ + c_3 \exp(z_-(\omega)(u - u_\theta))], \\ u_r \le u \le u_\theta \\ \widehat{\rho} = k[-\exp(u - u_\theta) + \exp(u - u_r) \\ + c_1 \exp(z_+(\omega)(u - u_\theta)) + c_2 \exp(z_+(\omega)(u - u_r)) \\ + c_3 \exp(z_-(\omega)(u - u_\theta))], \quad u \le u_r. \quad (45)$$

First we use the second boundary condition, equation (21), to solve for c_2:

$$-k - c_2 k = 0 \quad \Longrightarrow \quad c_2 = -1. \qquad (46)$$

Next, solving (20) for c_3 in terms of c_1 we get

$$-k + kc_1 + kc_3 = 0 \quad \Longrightarrow \quad c_3 = 1 - c_1. \qquad (47)$$

Equation (23) is then used to solve for the first order response component $\widehat{r}(\omega)$:

$$-r_0\tau_e - k - kc_2 z_+(\omega) = -r_0 \widehat{r}(\omega)\tau_e \qquad (48)$$

$$\widehat{r}(\omega) = 1 + \frac{k}{r_0\tau_e}(1 - z_+(\omega)) = 1 - \frac{\sqrt{1 + 4i\omega\tau_e} - 1}{2i\omega\tau_e}. \qquad (49)$$

From the third boundary condition (22) we obtain:

$$-r_0\tau_e - k + kc_1 z_+(\omega) - kc_3 z_-(\omega) = -r_0 \widehat{r}(\omega)\tau_e \qquad (50)$$

Using equation (48), substituting for c_3 and c_2 and using $z_+(\omega) + z_-(\omega) = 1$ yields

$$kc_1 z_+(\omega) + kc_3 z_-(\omega) = -kc_2 z_+(\omega) \qquad (51)$$

$$c_1(z_+(\omega) - z_-(\omega)) = (z_+(\omega) - z_-(\omega)) \Longrightarrow c_1 = 1 \qquad (52)$$

Substituting the values for the constants c_1, c_2, and c_3 into (45) yields the general solution given by equation (30).

7.2 Perturbations of the Mean

While holding σ^2 constant, let

$$\mu(t) = \mu_0(1 + \epsilon \exp(i\omega t)). \qquad (53)$$

The Fokker-Planck equation in the transformed coordinates is then

$$\tau_e \frac{\partial \rho(u,\omega)}{\partial t} = \frac{\partial \rho^2}{\partial^2 u} - (1 + \epsilon \exp(i\omega t))\frac{\partial \rho}{\partial u}. \qquad (54)$$

Breaking out the first order terms yields the nonhomogeneous differential equation:

$$\frac{d^2\widehat{\rho}}{du^2} - \frac{d\widehat{\rho}}{du} - i\tau_e \omega \widehat{\rho} = \frac{d\rho_0}{du}. \qquad (55)$$

Since $\frac{\partial^2 \rho_0}{\partial u^2} = \frac{\partial \rho_0}{\partial u}$, this equation differs from the corresponding variance equation (18) only in the sign of the nonhomogeneous term $d\rho_0/du$. Therefore, the same substitution, $\widehat{\rho}_p = K\frac{\partial \rho_0}{\partial u}$, can be used to find the particular solution

$$\widehat{\rho}_p = \frac{-1}{i\omega\tau_e}\frac{\partial \rho_0}{\partial u}. \qquad (56)$$

Furthermore, the homogeneous equation is identical to that for variance modulations and hence yields the same general solution. Equations (20), (21), and (24) remain the same for modulations in the mean. Equations (22) and (23) are replaced by:

$$\frac{\partial \widehat{\rho}}{\partial u}(u_\theta, \omega) = -r_0 \widehat{r}_\mu(\omega)\tau_e \qquad (57)$$

$$\frac{\partial \widehat{\rho}}{\partial u}(u_{r_+}, \omega) - \frac{\partial \widehat{\rho}}{\partial u}(u_{r_-}, \omega) = -r_0 \widehat{r}_\mu(\omega)\tau_e. \qquad (58)$$

Using these boundary conditions to solve for the constants in the general solution (Fourcaud and Brunel 2002), the firing rate modulations $\widehat{r}_\mu(\omega)$ are given by

$$\widehat{r}_\mu(\omega) = \frac{\sqrt{1 + 4i\omega\tau_e} - 1}{2i\omega\tau_e}. \qquad (59)$$

References

Abbott LF, Chance FS (2005) Drivers and modulators from push-pull and balanced synaptic input. ProgBrain Res 149:147–155

Abbott LF, van Vreeswijk C (1993) Asynchronous states in networks of pulse-coupled oscillators. Physical Review E 48(2):1483–1490

Abeles M (1991) Corticonics: Neural Circuits of the Cerebral Cortex. Cambridge University Press

Brunel N, Hakim V (1999) Fast global oscillations in networks of integrate-and-fire neurons with low firing rates. Neural Computation 11(7):1621–1671

Brunel N, Chance FS, Fourcaud N, Abbott LF (2001) Effects of synaptic noise and filtering on the frequency response of spiking neurons. Physical Review Letters 86(10):2186–2189

Calvin WH, Stevens CF (1967) Synaptic noise as a source of variability in the interval between action potentials. Science 155(764):842–844

Carandini M, Mechler F, Leonard CS, Movshon JA (1996) Spike train encoding by regular-spiking cells of the visual cortex. JNeurophysiol 76(5):3425–3441

Dodge J F A, Knight BW, Toyoda J (1968) Voltage noise in limulus visual cells. Science 160(823):88–90

Fourcaud N, Brunel N (2002) Dynamics of the firing probability of noisy integrate-and-fire neurons. Neural Computation 14(9):2057–2110

Fourcaud-Trocmé N, Brunel N (2005) Dynamics of the instantaneous firing rate in response to changes in input statistics. Journal of Computational Neuroscience 18(3):311–321

Frolov A, Medvedev A (1986) Substantiation of the 'point approximation' for describing the total electrical activity of the brain with the use of a simulation model. Biophysics 31:332–337

Fuortes MG (1959) Initiation of impulses in visual cells of limulus. JPhysiol 148:14–28

Gerstein GL, Mandelbrot B (1964) Random walk models for the spike activity of a single neuron. Biophysical Journal 4:41–68

Granit R (1947) Sensory Mechanisms of the Retina. Oxford University Press

Katz B (1950) Depolarization of sensory terminals and the initiation of impulses in the muscle spindle. JPhysiol 111(3-4):261–282

Knight BW (1972) Dynamics of encoding in a population of neurons. Journal of General Physiology 59(6):734–766

Knight BW, Toyoda JI, Dodge J F A (70) A quantitative description of the dynamics of excitation and inhibition in the eye of limulus. JGenPhysiol 56(4):421–437

Koch C (1999) Biophysics of Computation: Information Processing in Single Neurons. Oxford University Press, New York

Lindner B (2004) Interspike interval statistics of neurons driven by colored noise. PhysRevE StatNonlinSoftMatter Phys 69(2 Pt 1):022,901

Lindner B, Schimansky-Geier L (2001) Transmission of noise coded versus additive signals through a neuronal ensemble. Physical Review Letters 86(14):2934–2937

Miller KD, Troyer TW (2002) Neural noise can explain expansive, power-law nonlinearities in neural response functions. JNeurophysiol 87(2):653–659

Naundorf B, Geisel T, Wolf F (2005) Action potential onset dynamics and the response speed of neuronal populations. Journal of Computational Neuroscience 18(3):297–309

Nykamp DQ, Tranchina D (2000) A population density approach that facilitates large-scale modeling of neural networks: analysis and an application to orientation tuning. Journal of Computational Neuroscience 8(1):19–50

Plesser HE, Geisel T (1999) Markov analysis of stochastic resonance in a periodically driven integrate-and-fire neuron. Physical Review E 59(6):7008–7017

Ricciardi L (1977) Lecture Notes in Biomathematics. Springer-Verlag, Heidelberg, Germany

Salinas E, Sejnowski TJ (2002) Integrate-and-fire neurons driven by correlated stochastic input. Neural Computation 14(9):2111–2155

Silberberg G, Bethge M, Markram H, Pawelzik K, Tsodyks M (2004) Dynamics of population rate codes in ensembles of neocortical neurons. Journal of Neurophysiology 91(2):704–709

Stein RB, French AS, Holden AV (72) The frequency response, coherence, and information capacity of two neuronal models. BiophysJ 12(3):295–322

Troyer TW (06) Factors affecting phase synchronization in integrate-and-fire oscillators. JComputNeurosci 20(2):191–200

Troyer TW, Miller KD (1997) Physiological gain leads to high isi variability in a simple model of a cortical regular spiking cell. Neural Computation 9(5):971–983

Tuckwell HC (1988) Introduction to Theoretical Neurobiology: Volume 2. Cambridge University Press

Wilson HR, Cowan JD (1973) A mathematical theory of the functional dynamics of cortical and thalamic nervous tissue. Kybernetik 13(2):55–80